

Surface phonon spectroscopy of Ni(111) studied by inelastic electron scattering

W. Menezes,* P. Knipp,[†] G. Tisdale,[†] and S. J. Sibener*

The James Franck Institute, The University of Chicago, 5640 South Ellis Avenue, Chicago, Illinois 60637

(Received 9 November 1989)

We report the experimental determination and theoretical analysis of the surface phonon dispersion relations for clean Ni(111) along the $\bar{\Gamma}\bar{M}$ symmetry direction. The surface phonon spectra were obtained with a high-resolution electron energy loss spectrometer operating in the off-specular impact scattering regime. Kinematic conditions were varied in order to selectively examine the Rayleigh mode and "gap" mode, as well as contributions from bulk phonons. Comparison of the experimental surface phonon dispersion relations and inelastic scattering cross sections with lattice dynamical and quantum multiple scattering calculations demonstrate that tensile surface stress is present at the level of 1.6 ± 0.2 N/m, and that the intraplanar surface force constant is $(11 \pm 3)\%$ softer than in bulk nickel.

One of the central concerns in surface science today is to ascertain how the properties (static and dynamic) of surfaces differ from those of bulk matter. A very direct way to explore the dynamical aspects of this problem is to study the interatomic force constants in the vicinity of a surface. Two complementary experimental techniques currently exist for such studies: inelastic thermal helium atom scattering¹ and high-resolution electron energy loss spectroscopy (HREELS).² Helium atom scattering has superior energy resolution (200–500 μeV) and is surface specific, while HREELS can more easily probe higher energy surface vibrations and dipole-active modes. Both of these probes have scattering cross sections which vary strongly with incident beam energy and scattering geometry. Moreover, the energy-dependent inelastic electron scattering cross sections vary differently for different vibrational modes, allowing one to optimize the sensitivity to a specific spectral feature in a given scattering measurement.

In this paper we report on the surface dynamical properties of clean Ni(111) as examined by HREELS operating at high incident energies, in the off-specular impact scattering regime. The experimental results are analyzed using lattice dynamical and multiple scattering calculations. Ni(111) presents an excellent opportunity for studying the dynamical properties of a closest-packed surface which has nearly ideal termination with respect to its bulk geometry. Bulk nickel dispersion curves are fit extremely well by a simple force-constant model which assumes that the interatomic potential $\phi(r)$ is only nonzero between nearest neighbors.³ The first and second derivatives ϕ' and ϕ'' dictate the harmonic vibrations. (However, from total-energy minimization, ϕ' vanishes for this model.) Deviations of dynamical surface properties from "ideal termination" can be expressed in terms of $\phi_{ij}(r) \neq \phi(r)$, where $\phi_{ij}(r)$ is the (nearest-neighbor) potential between atoms in layers i and j . Previous studies^{4,5} indicate that the geometrical spacing between this unreconstructed surface and the second layer is within 1% of the bulk value. Hence, $\phi_{ij}(r) - \phi(r)$ is expected to be small.

We have observed the Rayleigh mode (S_1), "gap" mode (S_2), and contributions from bulk modes, i.e., surface resonances, (R_1) at several points along the $\bar{\Gamma}\bar{M}$ azimuth. Near $\bar{Q} = \bar{M}$, S_1 and S_2 are primarily localized in the surface layer and polarized shear vertically (SV) and longitudinally, respectively. Previous helium atom scattering experiments on the (111) surfaces of copper,⁶ silver,^{6,7} and platinum⁸ indicated 50%, 50%, and 40% softenings, respectively, of the intraplanar surface force constant ϕ''_{11} . However, these studies could not probe S_2 . Owing to its longitudinal polarization, S_2 is very sensitive to ϕ''_{11} . Recent Cu(111) HREELS experiments⁹ which could probe S_2 demonstrated surface phonon characteristics which required only 15% softening, consistent with a recent "embedded atom method" calculation.¹⁰ Owing to its SV polarization, S_1 is sensitive to both the interplanar force constant ϕ''_{12} and the surface stress ϕ'_{11} (from equilibrium considerations, ϕ'_{12} vanishes). This has been demonstrated for Ni(100),¹¹ Ni(110),¹² and Cu(100).¹³ Only in the case of Ni(110) was the existence of surface stress unambiguous. Previous neon atom scattering studies of Ni(111) (Ref. 14) mapped S_1 60% of the way from $\bar{\Gamma}$ to \bar{M} , although the spectra were complicated by multiphonon effects. In addition, their inability to probe zone-boundary phonons greatly decreased their sensitivity to the surface force field. Ibach *et al* used dipole HREELS to examine the folded substrate phonon modes at $\bar{\Gamma}$ for ordered overlayers of oxygen on Ni(111).¹⁵ Detailed calculations for the O/Ni system suggested that the observed frequencies were consistent with a lattice-dynamical model that assumed the surface force field to be unchanged from the bulk.¹⁶ However, it is unclear what relevance these results bear upon *clean* Ni(111).

Our surface-phonon measurements were carried out in a new electron scattering instrument which uses 127° cylindrical deflection optics. It consists of a fixed geometry double-pass monochromator and a rotating single-pass analyzer.¹⁷ The analyzer rotates in the scattering plane, covering the angular range 82°–137° with respect to the monochromator. The scattering plane includes the sur-

face normal. The instrumental resolution was 5–6 meV over the entire (1–250 eV) range. The in-plane angular width of the specular low-energy electron diffraction (LEED) beam, as measured with the rotating HREELS analyzer, was 1.5° . This width contains contributions from both the finite domain size of the surface and the instrument transfer function of the electron spectrometer. It corresponds to a momentum transfer resolution of $\pm 0.04 \text{ \AA}^{-1}$ for typical experimental configurations. The detector angle could be reproducibly positioned to within 0.1° .

The Ni(111) single crystal was polished to $0.05 \mu\text{m}$ and cut to within 0.5° of the desired orientation. This was confirmed using Laue x-ray backreflection. The $\bar{\Gamma}\bar{M}$ azimuthal orientation was selected by rotating the crystal until the $(0\bar{1})$ diffraction rod was detected with the HREELS analyzer. LEED I - V profiles established the absolute azimuthal orientation of the crystal. The crystal was cleaned by cycles of Ar^+ bombardment followed by annealing at 1000 K. Auger analysis verified surface cleanliness, while sharp LEED beams and low diffuse elastic scattering indicated the success of our annealing procedure. Crystal temperature was monitored with a type- K thermocouple that was spot welded to the side of the crystal. The base pressure in the crystal chamber was typically 5×10^{-11} Torr during data acquisition. Liquid nitrogen cooling of the target mount permitted data collection with surface temperatures as low as $T_s = 110$ K.

The cross sections for single-phonon scattering depend nontrivially on the impact energy E_i and experimental geometry (θ_i, θ_f) , exhibiting strongly nonmonotonic dependence on these parameters. An extensive parameter search has been used to identify conditions that optimize scattering contributions from selected vibrational features. Figure 1 shows three spectra which, from top to bottom, have been optimized for S_1 , S_2 , and R_1 contributions, respectively. The energy widths of S_1 and S_2 are consistent with the specular width of 5.5 meV. The peak positions and widths do not change as T_s is varied from 110 to 300 K; i.e., anharmonic effects are minimal. The intensity ratio of phonon creation and annihilation peaks equals the Boltzmann factor $\exp(\Delta E/k_B T)$. The multiphonon background tends to decrease with decreasing temperature and impact energy, making the lower temperature more desirable for most measurements. Various parallel momentum transfers \bar{Q} were accessed by rotating the analyzer while keeping the incident kinematics fixed, thereby mapping spectral features along the $\bar{\Gamma}\bar{M}$ azimuth. These measurements were primarily made in the second surface Brillouin zone (SBZ) towards the surface normal, since the intensities were approximately two to three times higher than in the first SBZ.¹¹

Figure 2 shows the dispersion relations for the Ni(111) surface phonons plotted as a function of the reduced parallel momentum transfer $\zeta \equiv Q/K_{\bar{M}}$, where $K_{\bar{M}} = 1.457 \text{ \AA}^{-1}$. For small Q , the dispersion relation $\omega = c_R Q$ is expected, where the Rayleigh wave velocity $c_R = 2780$ m/sec is calculated from the elastic constants of nickel.¹⁸ The data points for S_1 lie higher in energy than expected from the dispersion relation generated by a Green's-function calculation¹⁹ which assumes that the

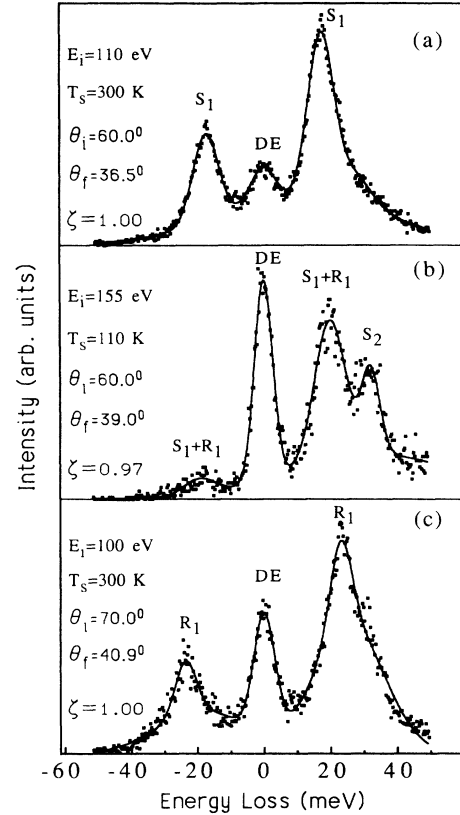


FIG. 1. Energy-loss spectra along the $\bar{\Gamma}\bar{M}$ direction which have been optimized for sensitivity to the (a) Rayleigh wave, S_1 ; (b) gap mode, S_2 ; (c) surface resonance, R_1 . DE represents the diffuse elastic scattering component. The solid lines are fits using sums of Gaussians.

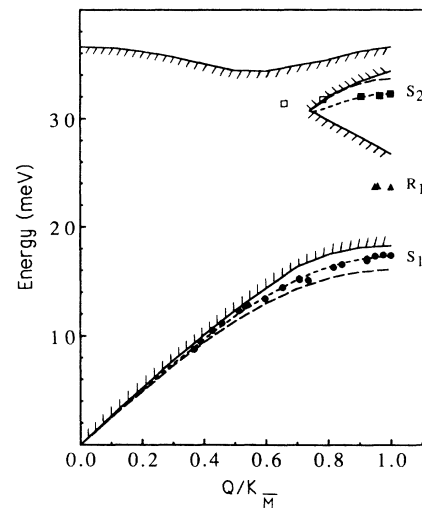


FIG. 2. Surface-phonon dispersion along the $\bar{\Gamma}\bar{M}$ direction. The uncertainty of the data is typically $\Delta E = \pm 0.3$ meV, $\Delta \zeta = \pm 0.01$, and $\Delta E = \pm 0.6$ meV for R_1 . Long-dashed lines are the lattice-dynamics results for S_1 and S_2 using as input the bulk force constant, whereas the short-dashed lines are for 11% intraplanar softening and 1.6 N/m tensile surface stress. Solid lines with cross hatching indicate the boundaries of the bulk phonon bands. At \bar{M} , the values of S_1 , S_2 , and R_1 are 17.2, 32.2, and 23.1 meV, respectively.

surface force constants are unchanged from the bulk value. Such a “surface phonon anomaly” requires the use of modified surface force constants (specifically ϕ''_{12} and/or ϕ''_{11}) to reconcile experiment and theory. However, arguments based on Badger’s rule,²⁰ which correlates bond-length variation [$\leq 1\%$ for Ni(111)] and force-constant change, discourage sizable modification in ϕ''_{12} to fit our data for S_1 . Instead, we get a good fit by assuming a tensile (attractive) surface stress with $\phi''_{11}/r = +(1.6 \pm 0.2)$ N/m, where $r = 2.49/\text{\AA}$ is the Ni-Ni distance (Fig. 2, short-dashed curve). For comparison, Table I lists the surface stresses for Ni(111), Ni(100), and Ni(110), all of which should be compared to the bulk nickel force constant $\phi'' = 37.6$ N/m. A correlation is evident between surface stress and the packing density of the topmost layer.

Owing to the non-Born nature of the electron-crystal interaction, the EELS intensities for various modes and their relative ratios depend quite sensitively on the experimental parameters (E_i , θ_i , and θ_f). As a result, it is possible to resolve S_2 in select configurations. For instance, Fig. 1(b) shows the energy-resolved intensity for $E_i = 155$ eV, $\theta_i = 60.0^\circ$, and $\theta_f = 39.0^\circ$ ($\zeta = 0.97$). [Curiously, scattering from the gap mode on another nickel surface, Ni(100), was also optimized at $E_i = 155$ eV.²¹] Quantum scattering calculations and experiments show the broad peak at ~ 20 meV to be an unresolved doublet composed of both S_1 and bulk (R_1) contributions. S_2 was mapped at several points in the gap near \bar{M} . The ratio of the integrated intensities of the S_2 peak to the $S_1 + R_1$ peak increases as one moves away from \bar{M} . Contrary to the S_1 findings, the data for S_2 lie lower in energy than the dispersion relation generated with the simple lattice-dynamical model (Fig. 2, long-dashed curve). The best agreement between the theoretical and experimental dispersion curves for S_2 is attained when ϕ''_{11} is softened by $(11 \pm 3)\%$ (Fig. 2, short-dashed curve), reminiscent of the Cu(111) results.⁹

One might contest that the single force constant model used here is too simplistic, thereby invalidating our results. Black *et al.*²² calculated the surface phonons for Ni(111), using a sizable assortment of interatomic potentials fitted to neutron scattering data and assumed to persist unchanged near the surface. For each model used, $S_1(\bar{M}) < 16.2$ meV and $S_2(\bar{M}) > 33.1$ meV. Since our values (17.2 ± 0.3 meV and 32.2 ± 0.3 meV) fall well outside of these limits, the effects of surface force field relaxation are unambiguous.

TABLE I. Nickel surface stresses.

Miller index	Direction	Surface packing density (r^{-2})	ϕ'/r^a (N/m)	Reference
(111)	$[1\bar{1}0]$	1.155	$+1.6 \pm 0.2$	This work
(001)	$[1\bar{1}0]$	1.000	+1.9	Ref. 12
(110)	$[1\bar{1}0]$	0.707	+3.0	Ref. 12
(110)	$[001]$	0.707	+4.2	Ref. 12

^aFor comparison, the bulk nickel force constant $\phi'' = 37.6$ N/m.

To confirm our spectroscopic findings, we have also performed quantum scattering calculations. The rigid-ion multiple-scattering method²¹ generated inelastic matrix elements which were combined²³ with vibrational spectral densities to yield the (unnormalized) single phonon cross section. To this were added a δ function in the elastic channel to simulate the diffuse scattering from defects and impurities, and a two-parameter Gaussian in order to approximate multiphonon contributions. The total was convoluted with the instrument transfer function to compare directly with experiment. Figures 3(a) and 3(b) show such fits to the data presented in Figs. 1(a) and 1(b), yielding best fit parameters of 1.6 N/m and 11% for the surface stress and intraplanar softening, respectively, in agreement with our (independent) spectroscopic conclusions.

In addition to scattering from true surface modes such as S_1 and S_2 , HREELS measurements can also contain contributions from bulk phonons.²⁴ In the top layer of the crystal, bulk and surface phonons contribute to the vibrational spectral density in roughly equal amounts. Deeper inside the crystal, bulk modes dominate the vibrational behavior. Because electrons can penetrate a few layers into the bulk before being inelastically scattered, their interactions can accordingly be dominated by bulk phonons under suitable conditions. Figure 1(c) shows a spectrum taken with $E_i = 100$ eV, $\theta_i = 70.0^\circ$, and $\bar{Q} = \bar{M}$ which has intense energy loss and gain features centered around 23 meV. These peaks, labeled as R_1 in Fig. 2, reside in the bulk band, so cannot be attributed to surface phonons. The R_1 scattering was intense only in a small angular range around \bar{M} . This abrupt appearance of R_1 differs from the behavior of the “longitudinal resonance” discussed in previous studies,^{6–10} which was seen to disperse across the surface Brillouin zone, approaching

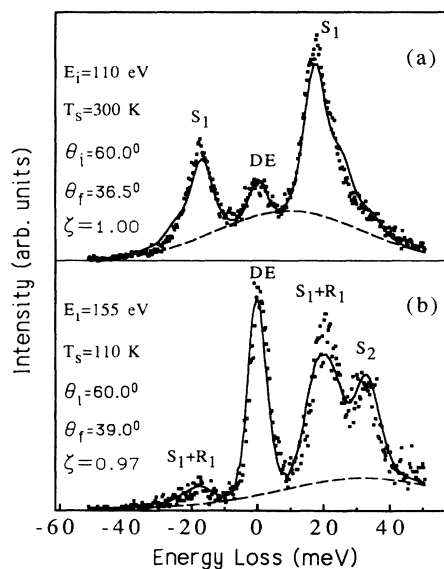


FIG. 3. Scattering calculations for the spectra shown in Figs. 1(a) and 1(b). The dashed line in each panel represents the estimated multiphonon contribution.

zero linearly at $\bar{\Gamma}$. Our attempts to fit quantitatively the scattering data for R_1 were poor; therefore we have not attempted to extract surface information from it.

To summarize, these results demonstrate that the surface force field for Ni(111) differs from expectations based upon simple extrapolation from bulk behavior. The intraplanar surface force constant is approximately 11% softer than in bulk nickel. In addition, tensile surface stress is present at the level of +1.6 N/m, indicating that the surface atoms have a desire to be more closely spaced than in the bulk. This level of stress has been predicted theoretically for a number of metal surfaces.²⁵ These surface force field assignments were derived from lattice dynamical fits to the spectroscopic results, and were independently confirmed by multiple-scattering calculations. Such calculations show that the scattering peaks are sensitive to the lattice dynamical model used, both in position and intensity. By varying the experimental parameters, we were able to resolve the different phonon

features as desired. It is hoped that the precision surface phonon measurements that are now available for Ni(111) will stimulate improved *ab initio* calculations on this interface.

We are extremely grateful to Helmut Krebs and the University of Chicago Machine Shop for their technical assistance. We wish to thank Ugo Fano for stimulating discussions and critical readings of the manuscript. We also wish to thank Burl Hall and Doug Mills for their scattering computer code and for numerous helpful conversations. This work was supported, in part, by the U.S. Air Force Office of Scientific Research, Grants No. AFOSR-84-0073 and No. AFOSR-88-0194; by the U.S. Department of Defense University Research Instrumentation Program; and by the National Science Foundation Materials Research Laboratory at the University of Chicago, Grant No. NSF-DMR-88-19860.

*Also at the Department of Chemistry, The University of Chicago, 5640 South Ellis Avenue, Chicago, IL 60637.

†Also at the Department of Physics, The University of Chicago, 5640 South Ellis Avenue, Chicago, IL 60637.

¹K. D. Gibson and S. J. Sibener, *J. Chem. Phys.* **88**, 7862 (1988); **88**, 7893 (1988).

²H. Ibach and D. L. Mills, *Electron Energy Loss Spectroscopy and Surface Vibrations* (Academic, New York, 1982).

³R. J. Birgeneau, J. Cordes, G. Dolling, and A. D. B. Woods, *Phys. Rev.* **136**, A1359 (1964).

⁴T. Narusawa, W. M. Gibson, and E. Törnqvist, *Surf. Sci.* **114**, 331 (1982).

⁵J. E. Demuth, P. M. Marcus, and D. W. Jepsen, *Phys. Rev. B* **11**, 1460 (1975).

⁶U. Harten, J. P. Toennies, and Ch. Wöll, *Faraday Discuss. Chem. Soc.* **80**, 137 (1985).

⁷V. Bortolani, A. Franchini, F. Nizzoli, and G. Santoro, *Phys. Rev. Lett.* **52**, 429 (1984).

⁸K. Kern, R. David, R. L. Palmer, G. Comsa, and T. S. Rahman, *Phys. Rev. B* **33**, 4334 (1986).

⁹Mohamed H. Mohamed, L. L. Kesmodel, Burl M. Hall, and D. L. Mills, *Phys. Rev. B* **37**, 2763 (1988); Burl M. Hall, D. L. Mills, Mohamed H. Mohamed, and L. L. Kesmodel, *ibid.* **38**, 5856 (1988).

¹⁰J. S. Nelson, M. S. Daw, and Erik C. Sowa, *Phys. Rev. B* **40**, 1465 (1989). There are numerous typographical errors in Table I of this reference.

¹¹S. Lehwald, J. M. Szeftel, H. Ibach, T. S. Rahman, and D. L.

Mills, *Phys. Rev. Lett.* **50**, 518 (1983).

¹²S. Lehwald, F. Wolf, H. Ibach, Burl M. Hall, and D. L. Mills, *Surf. Sci.* **192**, 131 (1987).

¹³M. Wuttig, R. Franchy, and H. Ibach, *Z. Phys. B* **65**, 71 (1986).

¹⁴B. Feuerbacher and R. F. Willis, *Phys. Rev. Lett.* **47**, 526 (1981).

¹⁵H. Ibach and D. Bruchmann, *Phys. Rev. Lett.* **44**, 36 (1980).

¹⁶V. Bortolani, A. Franchini, F. Nizzoli, and G. Santoro, *Solid State Commun.* **41**, 369 (1982).

¹⁷Electron optics fabricated by LK Industries, modified to allow analyzer rotation.

¹⁸G. W. Farnell, *Physical Acoustics VI*, edited by Warren P. Mason and R. N. Thurston (Academic, New York, 1970), p. 109.

¹⁹J. E. Black, Talat S. Rahman, and D. L. Mills, *Phys. Rev. B* **27**, 4072 (1983).

²⁰Richard M. Badger, *J. Chem. Phys.* **2**, 128 (1943).

²¹Mu-Liang Xu, B. M. Hall, S. Y. Tong, M. Rocca, H. Ibach, and S. Lehwald, *Phys. Rev. Lett.* **54**, 1171 (1985).

²²John E. Black and R. F. Wallis, *Phys. Rev. B* **29**, 6972 (1984); J. E. Black, F. Shanes, and R. F. Wallis, *Surf. Sci.* **133**, 199 (1983).

²³P. Knipp and Burl M. Hall, *Surf. Sci.* **224** (1990).

²⁴M. Rocca, S. Lehwald, H. Ibach, and Talat S. Rahman, *Surf. Sci.* **171**, 632 (1986).

²⁵M. C. Payne, N. Roberts, R. J. Needs, M. Needels, and J. D. Joannopoulos, *Surf. Sci.* **211/212**, 1 (1989).